The influence of nanoscale morphology on the resistivity of cluster-assembled nanostructured metallic thin films

2010 New J. Phys. 12 073001

(http://iopscience.iop.org/1367-2630/12/7/073001)

New Journal of Physics
The open-access journal for physics

The influence of nanoscale morphology on the resistivity of cluster-assembled nanostructured metallic thin films

E Barborini[1,3], G Corbelli[2], G Bertolini[1], P Repetto[1], M Leccardi[1], S Vinati[1] and P Milani[2,3]

[1] Tethis srl, via Franco Russoli 3, 20143 Milano, Italy
[2] CIMAINA and Dipartimento di Fisica, Università di Milano, via Celoria 16, 20133 Milano, Italy
E-mail: emanuele.barborini@tethis-lab.com and pmilani@mi.infn.it

New Journal of Physics **12** (2010) 073001 (12pp)
Received 13 March 2010
Published 1 July 2010
Online at http://www.njp.org/
doi:10.1088/1367-2630/12/7/073001

Abstract. We have studied *in situ* the evolution of the electrical resistivity of Fe, Pd, Nb, W and Mo cluster-assembled films during their growth by supersonic cluster beam deposition. We observed resistivity of cluster-assembled films several orders of magnitude larger than the bulk, as well as an increase in resistivity by increasing the film thickness in contrast to what was observed for atom-assembled metallic films. This suggests that the nanoscale morphological features typical of ballistic films growth, such as the minimal cluster–cluster interconnection and the evolution of surface roughness with thickness, are responsible for the observed behaviour.

Contents

[3] Authors to whom any correspondence should be addressed.

1. Introduction

The assembly of atomic clusters produced in the gas phase is considered a powerful bottom-up approach for the engineering of nanostructured thin films with tailored properties, since it allows, in principle, the control of the physical and chemical characteristics of the building blocks [1]–[3]. The survival of the nanoscale building blocks during the assembly process is called 'memory effect' and it can have a deep influence on the electrical and magnetic properties of the cluster-assembled systems, such as metallic thin films and wires [1, 2]. In particular, the electrical conductivity of cluster-assembled films may differ significantly with respect to the conductivity of atom-assembled films, due to the presence of nanoscale disorder and finite size effects [4]–[7].

Several authors have studied the evolution of electrical conduction in cluster-assembled films at very low coverage close to the percolation threshold [4]–[7]. However, the effects on the electrical conduction related to cluster–surface interaction, fragmentation, diffusion, cluster–cluster coalescence or sticking after the percolation onset and the first stage of three-dimensional (3D) growth remain almost completely unexplored. This is quite surprising, since there are many technological applications where the understanding and control of the influence of the nano- and mesostructure on the electrical properties of cluster-assembled thin films are crucial. Among them, one of the most popular is gas sensing through conductimetric microdevices. In these sensors, the presence of chemical species in air is detected through variations in the electrical conduction of a nanostructured layer with a large free-surface area and porosity [8]–[12].

The dependence of electrical resistivity on the dimensions of atom-assembled metallic thin films and wires has been systematically characterized due to the need for the extremely high integration of devices and hence the reduction in the dimensions of interconnects [13]–[16]. In these systems, the grain-boundary and surface scattering are known to increase the electrical resistivity when the lateral dimensions are scaled down to length scales (< 100 nm) comparable to the electronic mean free path [13].

In their seminal work, Fuchs and Sondheimer [17, 18] modelled the resistivity increase in thin films as related to diffuse scattering at the film boundaries, which essentially imposes a restriction on the electronic mean free path. Since the resistivity is inversely proportional to the mean free path, it consequently increases. In the Fuchs–Sondheimer theory, the surface of thin films is the only confinement structure playing a morphology-related additional role in electron scattering. Hence, the model provides good explanations of single-crystal thin film resistivity.

Further theoretical developments considered other morphology-related structures contributing to electron scattering, such as grain boundaries and surface roughness [19]–[25]. In particular, Mayadas and Shatzkes [19] attributed the enhanced resistivity of thin films to grain boundary scattering superimposed on the smaller Fuchs–Sondheimer size effect. The key idea of their work lies in the observation that, up to film thicknesses of the order of 1 μm, the mean grain diameter is approximately equal to the film thickness, due to the growth mechanism of atom-assembled thin films [26].

Cluster-assembled films have a growth mechanism substantially different from that of atom-assembled ones, so a different relationship between their electrical conduction properties, morphology and growth dynamics should be expected. We have investigated the evolution, with thickness, of the electrical conduction of different metallic cluster-assembled films, measured *in situ* during the film growth.

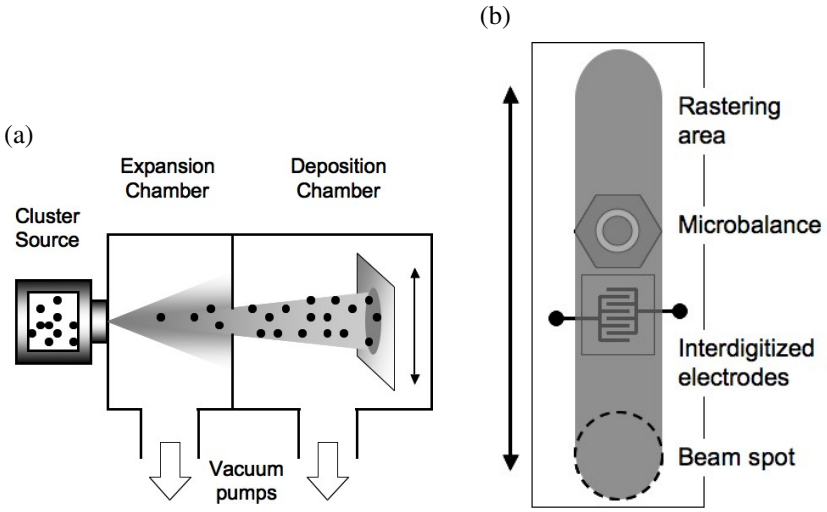

Figure 1. (a) Scheme of an SCBD apparatus. Driven by the pressure difference, a supersonic expansion of argon occurs, generating a beam that carries clusters from the cluster source towards the deposition chamber. Here a motorized sample holder provides for substrate rastering (arrows) to ensure uniform coverage. (b) Detail of the experimental setup part that collects clusters and is dedicated to the measurement of thickness and electrical conduction. The former is performed by a quartz crystal microbalance, and the latter by a pair of interdigitized electrodes. The real beam spot and rastered area are much larger than in the drawing.

2. Experimental

Cluster-assembled metallic thin films were produced by supersonic cluster beam deposition (SCBD) using an apparatus equipped with a pulsed microplasma cluster source (PMCS) [2, 27, 28] (figure 1(a)). The PMCS operates through the ablation of a metallic target by an argon plasma jet, ignited by a pulsed electric discharge. After ablation, metallic atoms thermalize with the inert gas and condense to form clusters. The inert gas–cluster mixture then expands through the nozzle, forming a seeded supersonic beam. A set of aerodynamic lenses [2, 29] mounted after the PMCS nozzle forces the clusters to concentrate close to the beam axis, increasing the beam collimation and the in-axis intensity. A differentially pumped deposition chamber hosts the substrate holder placed on the cluster beam axis. Clusters are deposited at room temperature with a kinetic energy per atom of a few tens of eV, thus preventing significant fragmentation of the aggregates. The use of a PMCS allows us to routinely achieve a very stable and regular deposition rate for a wide range of metals. In the present experiment, we produced Fe, Pd, Nb, W and Mo.

The evolution of the electrical conduction of cluster-assembled films was measured *in situ* during deposition on high-resistivity alumina substrates with an interdigitized electrode pair with ten platinum fingers each (2 mm in length, 50 μm width, 50 μm spacing and 280 nm thickness) connected to an electrometer with an internal voltage source (Keithley 6517A, applied voltage of 100 mV). Alumina substrates with both standard and high-grade surface polishing were used to take into account the role of substrate morphology. The cluster beam spot of a few cm in diameter was rastered on an *xyz* motorized sample holder, where the

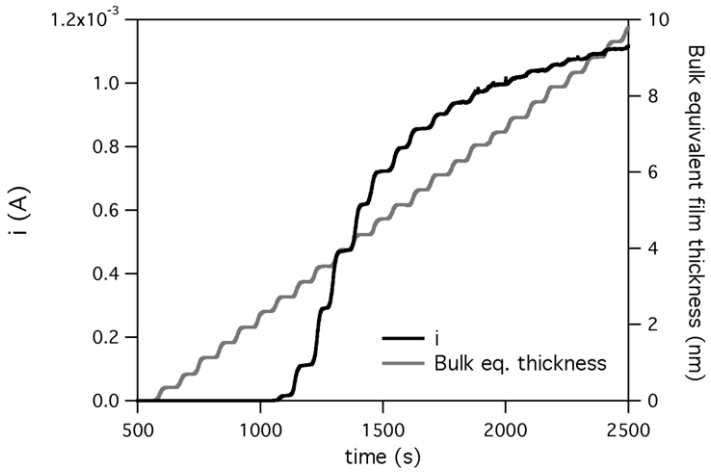

Figure 2. Raw data from the electrode pair (left axis) and quartz microbalance (right axis) during rastered deposition. In the time intervals when electrodes were not exposed to the cluster beam, it is possible to evaluate the effect of background gas on film conduction. The right axis label 'bulk equivalent film thickness' emphasizes that the microbalance measures the mass and converts it to thickness on the basis of bulk densities. The real thickness of non-compact materials is higher than 'bulk equivalent thickness', according to the bulk-film densities ratio.

alumina substrate was fixed close to a quartz microbalance in order to measure continuously the evolution of film thickness, as sketched in figure 1(b). The microbalance calculates the thickness by measuring the mass, for a given quartz sensor area and material density. The real thickness of non-compact films, such as the cluster-assembled ones of the present experiment, is higher than values reported by the microbalance, according to the bulk-film densities ratio. To emphasize this point, we will use the expression 'bulk equivalent film thickness' to indicate the measure of the microbalance.

Cluster beam rastering allows the deposition of several up-and-down stripes of the material over an area significantly larger than that occupied by the alumina substrate with interdigitated electrodes and the microbalance, thus ensuring a uniform and identical coverage on both. Moreover, cluster beam rastering allows the characterization of the effect of background gas exposure, which is around 1×10^{-6} torr, on conduction (see below).

Figure 2 shows an example of raw conduction data obtained during the deposition of tungsten clusters. The step-like behaviour of both current and thickness evolution is related to the periodic deposition of the cluster beam on the interdigitated electrodes and microbalance due to the rastering.

3. Results and discussion

Figure 3(a) shows the typical morphology of W, Mo and Fe cluster-assembled films, measured *ex situ* by atomic force microscopy (AFM). Nb and Pd (not reported) show similar morphological features. The roughness and granularity of the films do not depend on the material, as also confirmed by scanning electron microscopy analysis (not shown). The observed

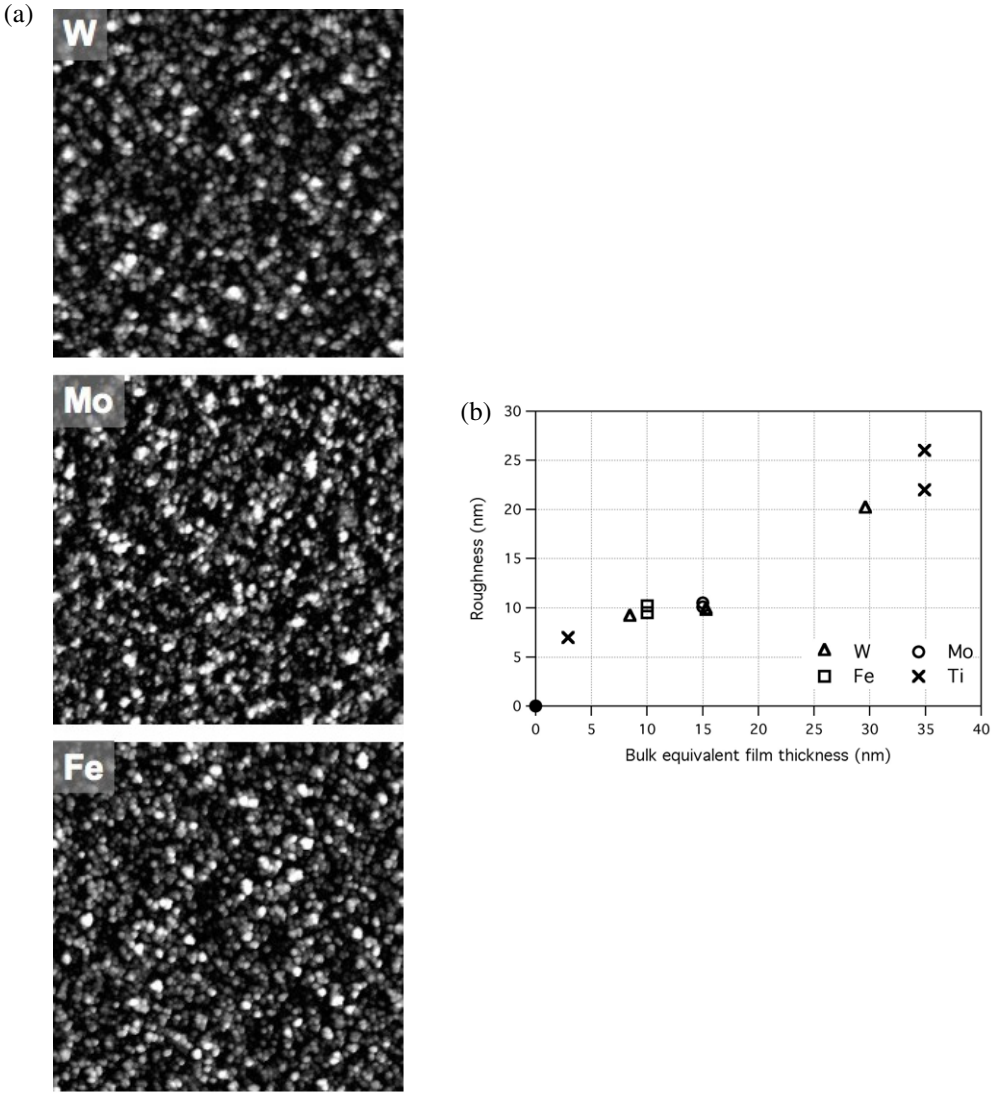

Figure 3. (a) Surface morphologies of cluster-assembled W, Mo and Fe by AFM (the side of the images correspond to 1 μm; the thickness of the films is a few tens of nm). The morphologies of W, Mo and Fe films look very similar, indicating similar cluster dimensions and similar growth dynamics. (b) Film roughness as a function of the thickness for the materials of (a). Although not included in the study of electrical conduction, data on cluster-assembled Ti films produced with the same technique have been added to the graph to demonstrate the general character of the roughness trend.

morphology can be ascribed to the ballistic growth regime [3, 30], which is characterized by nanoscale porosity, poorly connected and non-compact structures with lower density with respect to bulk, and increasing surface roughness with film thickness, as shown in figure 3(b).

The behaviour of the electrical current across the cluster-assembled films as a function of the thickness is reported in figure 4. We observe three distinct regimes: (i) no variation of the conduction upon film growth below a certain critical thickness; (ii) sharp onset of the conduction

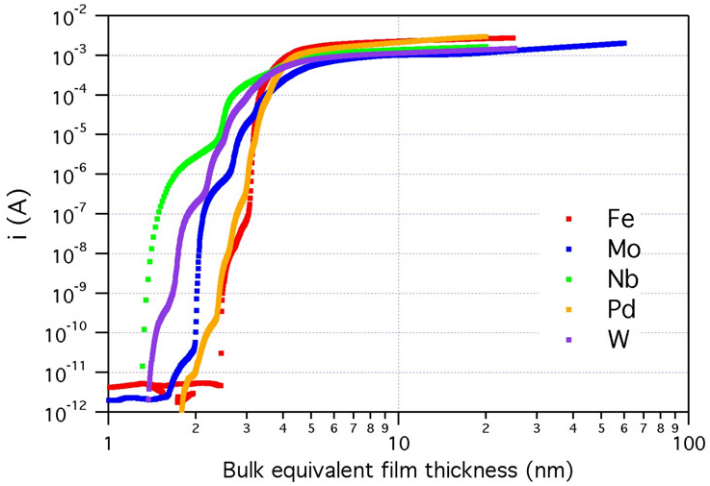

Figure 4. Measurements of the electrical current across the films as a function of the thickness. The log–log plot emphasizes the eight-order-of-magnitude increase in the current occurring in a few nm thickness range, and the nonlinear asymptotic trend. The current 'oscillations' occurring at the onset are artefacts due to the non-perfectly simultaneous exposition of the microbalance and electrode pair to the cluster beam.

characterized by an abrupt increase in the current of several orders of magnitude taking place in a narrow range of thicknesses; (iii) an asymptotic trend at greater thicknesses. The thickness values separating the different regimes are almost the same for all the metals.

These data were obtained on alumina with standard surface polishing. Measurements on alumina with high-grade surface polishing show a similar behaviour, except for a slightly smaller thickness at the current onset for all metals. The effect of background gas on the conduction of the growing films has been estimated in the time intervals of rastering protocol when the electrode pair is not exposed to the cluster beam. In these time intervals, the growing film is exposed to the background atmosphere only. Therefore, its role in conduction, and in particular the oxidation due to oxygen partial pressure, has been evaluated. In the case of Fe and Nb, the effect of oxidation is detectable through a slight current decrease, while in the case of Mo, W and Pd, no evidence of oxidation appeared during the experiment time scale.

Figure 5 shows the resistivity of cluster-assembled films calculated from the data reported in figure 4. The curves reveal, on the one side, resistivity values of 3–4 orders of magnitude higher than bulk ones for any metal at any thickness and, on the other side, a non-monotonic behaviour, with a local minimum around 5–6 nm. Remarkably, the resistivity of cluster-assembled films shows an increasing asymptotic trend with growing thickness instead of a decreasing trend converging to bulk values, as reported in the literature for atom-assembled films [13, 14, 16]. For all the metals, the resistivity increases according to a power law, as highlighted by the constant slope in the log–log plot. The calculated exponents of power law are 0.41 for Pd, 0.70 for W and 0.78 for Fe and Nb. The comparison of the resistivities at a given thickness shows that the relative behaviour of cluster-assembled materials may be different with respect to their bulk counterpart. For example, between 5 and 10 nm, Mo and W have resistivities higher than other metals, opposite to what happens in bulk.

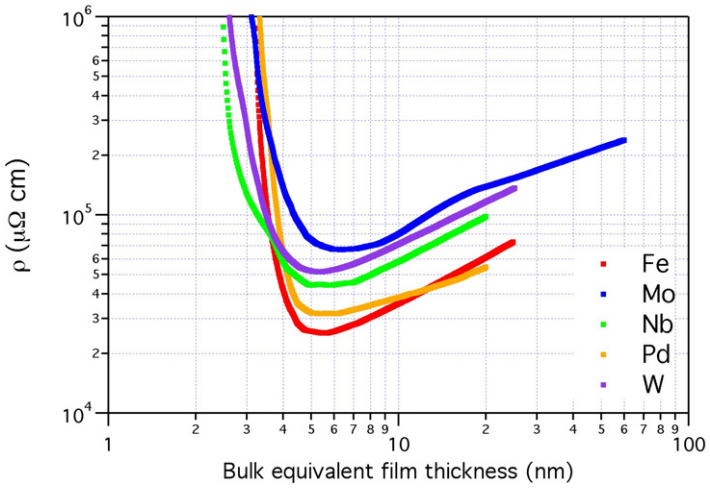

Figure 5. Resistivity of the cluster-assembled films as a function of film thickness. The non-monotonic behaviour can be ascribed to peculiar topological evolution occurring in the cluster-assembled film during growth (see text). The linear behaviour appearing as an asymptotic trend in the log–log plot indicates a power-law dependence. The calculated exponents are 0.41 for Pd, 0.70 for W and 0.78 for Fe and Nb.

The sharp onset of the conduction can be explained by the reaching of the percolation threshold ([31, 32]; [33] and references therein). Once the first percolation path among deposited clusters closes, the current begins to flow, and its huge increase is related to the increase in the paths becoming available for electron drifting as clusters progressively land and interconnect themselves, as shown schematically in figure 6. The geometry of the conduction through the cluster-assembled film, within a small range of thicknesses, evolves from 0D to 1D and then to 2D. The 0D–1D transition takes place at a sub-monolayer coverage corresponding to a mean thickness of 1–2 nm; the 1D–2D transition takes place between 1–2 and 3–4 nm. Once 2D conduction becomes saturated for the running out of in-plane conduction paths at 3–4 nm, conduction starts evolving from 2D to 3D. The increase in the current slows down and the resistivity reaches its minimum around 5–6 nm. At this point, 2D–3D transition is completed and the conduction within the film starts evolving in 3D structure.

We suggest that 2D–3D transition should occur within a few cluster layers. In a very simple model where a spheroidal shape is assumed for clusters, a few non-compact layers should have a mass corresponding to a compact layer with a thickness similar to the diameter of clusters responsible for the larger volume fraction. Hence, since the quartz microbalance measures the thickness through the measure of a mass (see section 2), 5–6 nm should be the cluster size dominating the volume fraction. These sizes are in pretty good agreement with AFM characterization of cluster size distribution, carried out on samples with sub-monolayer coverage. Figure 7 shows, as an example, the size distribution and the corresponding volume fraction for Fe clusters. As expected by the gas-phase synthesis process occurring in PMCS, the cluster size distribution is log-normal [3] and the volume fraction calculated on log-normal fit has a maximum around 5 nm.

Although film oxidation by background gas was observed in Fe and Nb, this cannot account for the huge resistivity discrepancy with respect to bulk, occurring to almost the same extent in

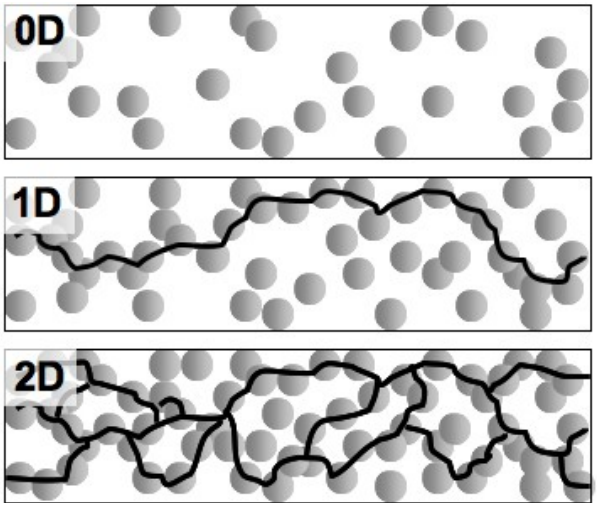

Figure 6. At early growth stages, clusters are separated from each other, preventing current from flowing (0D conductor). The sharp onset of the conduction occurs at the percolation threshold when the first path among deposited clusters closes (1D conductor). The huge conduction increase is due to the number of new paths becoming available as clusters progressively land and interconnect themselves (1D to 2D conductor). Nevertheless, a minimal contact area is expected for the low energy of the deposition process, limiting fragmentation, deformation and cluster–cluster coalescence.

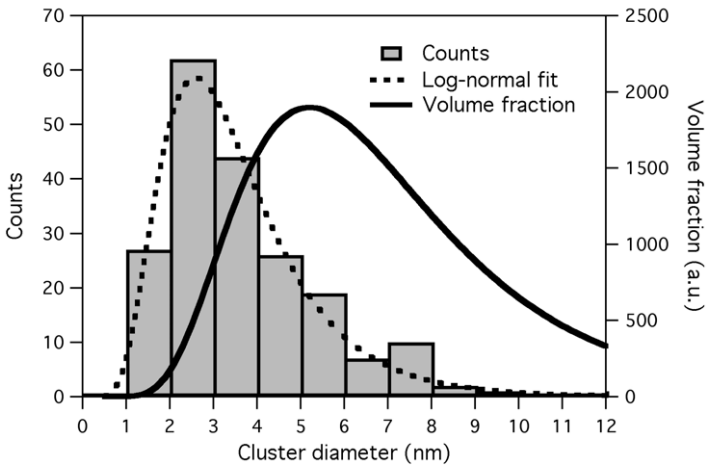

Figure 7. Cluster size distribution of Fe clusters obtained by AFM on samples with sub-monolayer coverage and log-normal fit (grey solid bars and dashed line, referring to the left axis). The log-normal distribution, expected by the gas-phase synthesis process of clusters occurring in PMCS, has a centre at 2.59 ± 0.05 nm and a width of 0.65 ± 0.02. On the basis of this curve, the corresponding volume fraction has been calculated (solid line, right axis).

all metals, and thus excluding the role of chemical modification in the observed resistivity trend, which is at odds with the trend modelled by the Fuchs–Sondheimer and Mayadas–Shatzkes models ([19]; [34] and references therein).

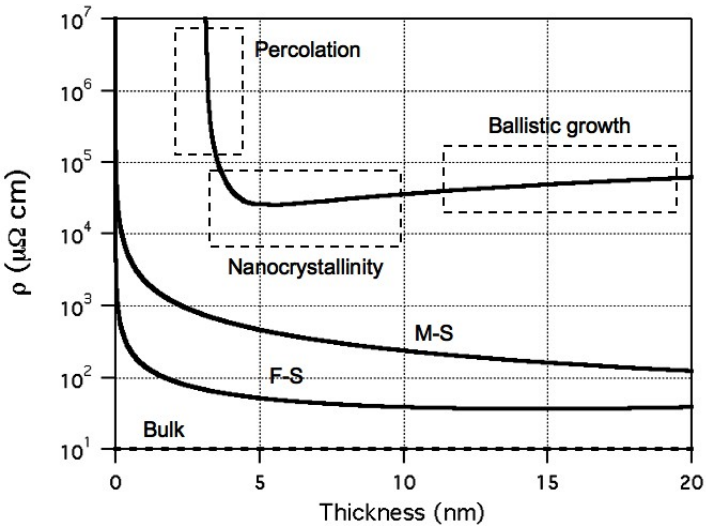

Figure 8. Evolution of the resistivity curves of Fe as nanoscale topological discontinuities are further added, from ideal bulk to ballistic growth of the cluster-assembled film, passing through the Fuchs–Sondheimer (F–S) and Mayadas–Shatzkes (M–S) modelled systems. F–S and M–S curves are obtained assuming $p = 0$ in F–S, and $p = 0$, $R = 0.8$, and grain size equal to thickness in M–S.

Figure 8 shows the resistivity as a function of the thickness in the case of cluster-assembled Fe thin film, compared with the ones modelled according to the Fuchs–Sondheimer and Mayadas–Shatzkes models. To account for large discrepancies, we suppose that the departure of cluster-assembled film resistivity from that of atom-assembled films can be understood by taking into account the hierarchical organization of different morphological elements. Nanosized building blocks, upon deposition, do maintain a substantial memory of their original structure and dimensions, while low cluster–cluster interaction, due to low-energy conditions of the deposition process, is expected to be at the base of percolative conduction, where paths available for electron drift are choked by small contact areas, even when the 3D regime has been reached.

The increasing asymptotic trend of resistivity can be explained by considering that cluster-assembled films show peculiar 3D growth dynamics ascribable to the ballistic regime, whose main characteristic, besides minimal grain interconnections, is the progressive decrease in the topological connection of the uppermost layers [30]. From this point of view, the trend of surface roughness, as shown in figure 3(b), is evidence for this feature. Hence, even if the same number of clusters are deposited during a given time, the contribution to electrical conduction gets lower and lower as the surface roughness increases. The uppermost layers of the growing film are less compact and hence less conductive due to the decreasing percolative path density caused by minimal cluster interconnection and morphologies related to the ballistic growth regime.

In other words, we suppose that resistivity behaviour could be ascribed to 3D growth dynamics and the related formation of percolation paths. A model trying to account for electrical conduction in such nanostructured media should consider how morphology parameters scale

during film growth [30] and how they could influence the site probability of percolation theory [31]. In the classical percolation problem, the site probability is proportional to film thickness or volume fraction. However, in cluster-assembled films, the configuration of the system changes with deposition time and, in particular, the network connectivity decreases as the surface roughness increases. In this case, the scaling behaviour of morphological parameters could influence the percolation site probability, leading to a more complex relation with film thickness. Although sophisticated models taking into account surface roughness and general morphological aspects, which could introduce additional scattering points, especially in ultrathin metal films, have been proposed [22, 23, 25], [35]–[37], to our knowledge, dynamic models that consider percolation phenomena during the film growth are not available in the literature.

We suppose that such an 'anisotropic' 3D percolation model, together with additional experimental investigations at high deposition temperatures, which should cause structure densification and cluster–cluster contact area increase, could highlight these hypotheses and help us to obtain a deeper knowledge of the electrical transport behaviour of cluster-assembled films with ballistic growth dynamics.

4. Conclusions

We have investigated *in situ* the evolution of the electrical transport properties of metallic cluster-assembled thin films during their growth. We observed that electrical conduction evolves according to nanoscale topological evolution of the films: from 0D to 1D when isolated clusters close the first percolative path; from 1D to 2D when new conduction paths develop as clusters are progressively added. After reaching the 3D regime, the resistivity of the cluster-assembled films increases with increasing thickness, in substantial disagreement with the bulk-converging behaviour observed for atom-assembled films in the same thickness range.

Ballistic growth accounts for minimal cluster–cluster contact area and increasing surface roughness. Nanocrystallinity, minimal contact area and nanoscale grain boundaries may explain the huge discrepancy between cluster-assembled and atom-assembled thin film resistivity evolutions, while surface roughness increase explains the non-constant resistivity asymptotic trend. All the studied metals showed similar behaviour, suggesting that conduction features are largely dominated by morphology, no matter what the material is. This is also supported by the comparison of the resistivities at a given thickness where the relative behaviour of cluster-assembled materials may be different with respect to their bulk counterpart.

From a technological point of view, our results show a bottom-up approach to the synthesis of nanomaterials from nanoscale building blocks, where the memory effect as well as a careful choice of deposition conditions and thicknesses range can be exploited to engineer the materials' properties. In particular, the influence of nanoscale morphology on the electrical resistivity is of relevance to the design of devices with electrical read-out, such as gas sensors, where nanostructured layers are used as active elements.

Acknowledgment

We thank A Podestà and M Indrieri for AFM characterization.

References

[1] Perez A *et al* 1997 Cluster assembled materials: a novel class of nanostructured solids with original structures and properties *J. Phys. D: Appl. Phys.* **30** 709

[2] Wegner K, Piseri P, Vahedi Tafreshi H and Milani P 2006 Cluster beam deposition: a tool for nanoscale science and technology *J. Phys. D: Appl. Phys.* **39** R439

[3] Milani P and Iannotta S 1999 *Cluster Beam Synthesis of Nanostructured Materials* (Berlin: Springer)

[4] Hihara T, Yamada Y, Katoh M, Peng D L and Sumiyama K 2003 Electron transport properties in Nb and NbN cluster-assembled films produced by a plasma-gas-condensation cluster source *J. Appl. Phys.* **94** 7594

[5] Yamamuro S, Sumiyama K, Hihara T and Suzuki K 1999 Geometrical and electrical percolation in nanometre-sized Co-cluster assemblies *J. Phys.: Condens. Matter* **11** 3247

[6] Jensen P, Melinon P, Hoareau A, Xiong Hu J, Cabaud B, Treilleux M, Bernstein E and Guillot D 1992 Experimental achievement of 2D percolation and cluster-cluster aggregation models by cluster deposition *Physica* A **185** 104

[7] Schmelzer J, Brown S A, Wurl A, Hyslop M and Blaikie R J 2002 Finite-size effects in the conductivity of cluster assembled nanostructures *Phys. Rev. Lett.* **88** 226802

[8] Graf M, Gurlo A, Barsan N, Weimar U and Hierlemann A 2006 Microfabricated gas sensor systems with sensitive nanocrystalline metal-oxide films *J. Nanopart. Res.* **8** 823

[9] Barborini E *et al* 2008 Batch fabrication of metal oxide sensors on micro-hotplates *J. Micromech. Microeng.* **18** 055015

[10] Favier F, Walter E C, Zach M P, Benter T and Penner R M 2001 Hydrogen sensors and switches from electrodeposited palladium mesowire arrays *Science* **293** 2227

[11] Dankert O and Pundt A 2002 Hydrogen-induced percolation in discontinuous films *Appl. Phys. Lett.* **81** 1618

[12] Xu T, Zach M P, Xiao Z L, Rosenmann D, Welp U, Kwok W K and Crabtree G W 2005 Self-assembled monolayer-enhanced hydrogen sensing with ultrathin palladium films *Appl. Phys. Lett.* **86** 203104

[13] Steinhögl W, Schindler G, Steinlesberger G, Traving M and Engelhardt M 2005 Comprehensive study of the resistivity of copper wires with lateral dimensions of 100 nm and smaller *J. Appl. Phys.* **97** 023706

[14] Lim J-W and Isshiki M 2006 Electrical resistivity of Cu films deposited by ion beam deposition: effects of grain size, impurities, and morphological defect *J. Appl. Phys.* **99** 094909

[15] Durkan C and Welland M E 2000 Size effects in the electrical resistivity of polycrystalline nanowires *Phys. Rev.* B **61** 14215

[16] Steinlesberger G, Engelhardt M, Schindler G, Steinhogl W, von Glasow A, Mosig K and Bertagnolli E 2002 Electrical assessment of copper damascene interconnects down to sub-50 nm feature sizes *Microlectron. Eng.* **64** 409

[17] Fuchs X K 1938 The conductivity of thin metallic films according to the electron theory of metals *Proc. Camb. Phil. Soc.* **34** 100

[18] Sondheimer E H 1952 The mean free path of electrons in metals *Adv. Phys.* **1** 1

[19] Mayadas A and Shatzkes M 1970 Electrical-resistivity model for polycrystalline films: the case of arbitrary reflection at external surfaces *Phys. Rev.* B **1** 1382

[20] Lucas M S P 1965 Electrical conductivity of thin metallic films with unlike surfaces *J. Appl. Phys.* **36** 1632

[21] Soffer S B 1967 Statistical model for the size effect in electrical conduction *J. Appl. Phys.* **38** 1710

[22] Namba Y 1968 Electrical conduction of thin metallic films with rough surface *J. Appl. Phys.* **39** 6117

[23] Elsom K C and Sambles J R 1981 Macroscopic surface roughness and the resistivity of thin metal films *J. Phys. F: Met. Phys.* **11** 647

[24] Fishman G and Calecki D 1989 Surface-induced resistivity of ultrathin metallic films: a limit law *Phys. Rev. Lett.* **62** 1302

[25] Fishman G and Calecki D 1991 Influence of surface roughness on the conductivity of metallic and semiconducting quasi-two-dimensional structures *Phys. Rev.* B **43** 11581

[26] Arnason S B, Herschfield S and Hebard A 1998 Bad metals made with good-metal components *Phys. Rev. Lett.* **81** 3936
[27] Barborini E, Piseri P and Milani P 1999 A pulsed microplasma source of high intensity supersonic carbon cluster beams *J. Phys. D: Appl. Phys.* **32** L105
[28] Milani P, Piseri P, Barborini E, Podestà A and Lenardi C 2001 Cluster beam synthesis of nanostructured thin films *J. Vac. Sci. Technol.* A **19** 2025
[29] Liu P, Ziemann P J, Kittelson D B and McMurray P H 1995 Generating particle beams of controlled dimensions and divergence: I. Theory of particle motion in aerodynamic lenses and nozzle expansions *Aerosol Sci. Technol.* **22** 293
[30] Barabasi A-L and Stanley H E 1995 *Fractal Concepts in Surface Growth* (Cambridge: Cambridge University Press)
[31] Stauffer D and Aharony A 1992 *Introduction to Percolation Theory* (London: Taylor and Francis)
[32] Morris J E and Coutts T J 1977 Electrical conduction in discontinuous metal films: a discussion *Thin Solid Films* **47** 3
[33] Nayak M, Lodha G S and Nandedkar R V 2006 Nucleation, growth, percolation, and amorphous to crystalline transition of ultrathin molybdenum films *J. Appl. Phys.* **100** 113709
[34] See, for instance, Camacho J M and Oliva A I 2005 Morphology and electrical resistivity of metallic nanostructures *Microelectron. J.* **36** 555
[35] Jacob U, Vancea J and Hoffmann H 1990 Surface-roughness contributions to the electrical resistivity of polycrystalline metal films *Phys. Rev.* B **41** 11852
[36] Luo E Z, Heun S, Kennedy M, Wollschläger J and Henzler M 1994 Surface roughness and conductivity of thin Ag films *Phys. Rev.* B **49** 4858
[37] Kaser A and Gerlach E 1995 Scattering of conduction electrons by surface roughness in thin metal films *Z. Phys. B: Condens. Matter* **97** 139